DAFD: Domain Adaptation via Feature Disentanglement for Image Classification

Zhize Wu, Changjiang Du, Le Zou, Ming Tan, Tong Xu, Fan Cheng, Fudong Nian, and Thomas Weise

***Abstract*—A good feature representation is the key to image classification. In practice, image classifiers may be applied in scenarios different from what they have been trained on. This so-called domain shift leads to a significant performance drop in image classification. Unsupervised domain adaptation (UDA) reduces the domain shift by transferring the knowledge learned from a labeled source domain to an unlabeled target domain. We perform feature disentanglement for UDA by distilling category-relevant features and excluding category-irrelevant features from the global feature maps. This disentanglement prevents the network from overfitting to category-irrelevant information and makes it focus on information useful for classification. This reduces the difficulty of domain alignment and improves the classification accuracy on the target domain. We propose a coarse-to-fine domain adaptation method called Domain Adaptation via Feature Disentanglement (DAFD), which has two components: (1) the Category-Relevant Feature Selection (CRFS) module, which disentangles the category-relevant features from the category-irrelevant features, and (2) the Dynamic Local Maximum Mean Discrepancy (DLMMD) module, which achieves fine-grained alignment by reducing the discrepancy within the category-relevant features from different domains. Combined with the CRFS, the DLMMD module can align the category-relevant features properly. We conduct comprehensive experiment on four standard datasets. Our results clearly demonstrate the robustness and effectiveness of our approach in domain adaptive image classification tasks and its competitiveness to the state of the art.**

***Index Terms*—Domain Shift, Domain Adaptation, Image Classification, Feature Selection.**

I. Introduction

When training deep neural networks for classification, the training and test sets stem from the same distribution. In practice, the networks may also be applied in different scenarios with significant discrepancies from the source domain, as illustrated in Figure 1. Such domain shifts [1] lead to drops in accuracy. Since the labelling of data is expensive, it is usually not feasible to have huge training sets covering many different domains. This led to the idea of unsupervised domain adaptation (UDA) [2], which aims to map feature vectors of different domains into a common feature space.

Fig. 1. Example of domain shift. The above images are from the Office-Home dataset [3]. The images in each row are selected from the same domain. The images in each column belong to the same category. While their categories are the same, the objects within a column differ greatly in appearance.

In [4], for instance, a dual stream model reduces the maximum mean discrepancy between the source and target domains. In [5], a Gradient Reversal Layer (GRL) and a domain classifier are used to implement domain confusion. The GRL creates domain-invariant features, i.e., ensures that the features of different domains are similar. Although such discrepancy-based UDA methods have achieved good results, they do not consider the entanglement of category-relevant and category-irrelevant features.

For image classification, the foreground plays an important role, while the background features are basically noise [6]. During the learning process, category-irrelevant features interfere with the proper alignment of the domains. Moreover, the background tends to take up most of the image. Consequently, the features extracted in typical discrepancy-based UDA methods contain a category-irrelevant bias and cannot be perfectly domain-invariant. As a result, UDA models perform tangibly worse on the target domain.

Therefore, several recent models for UDA object detection tasks try to disentangle the features. In [7], an attention-induced feature selection module exploits ground-truth bounding boxes to extract the areas relevant for classification. In [8], the Domain Disentanglement Faster-RCNN implements feature disentanglement and removes domain-specific features from the global features by using an Instance Similarity Disentanglement module and a Global Triplet Disentanglement module, respectively. However, in image classification

Zhize Wu is with the Institute of Applied Optimization, School of Artificial Intelligence and Big Data, Hefei University, and the Information Materials and Intelligent Sensing Laboratory of Anhui Province, Anhui University, Hefei, 230601, China. E-mail: wuzz@hfuu.edu.cn

Thomas Weise, Ming Tan, Le Zou, and Changjiang Du are with the Institute of Applied Optimization, School of Artificial Intelligence and Big Data, Hefei University, Hefei, 230601, China. E-mail: {tweise,tanming,zoule}@hfuu.edu.cn, ducj@stu.hfuu.edu.cn

Fudong Nian is with the School of Advanced Manufacturing Engingeering, Hefei University, Hefei, 230601, China. E-mail: niangfd@hfuu.edu.cn

Tong Xu is with the School of Computer Science and Technology, University of Science and Technology of China, Hefei, 230026, China. E-mail: tongxu@ustc.edu.cn

Fan Cheng is with the Information Materials and Intelligent Sensing Laboratory of Anhui Province, Anhui University, Hefei, 230601, China. E-mail: chengfan@mail.ustc.edu.cn

(Corresponding author: Thomas Weise.)

tasks, there are no ground-truth bounding boxes available during training. Thus, the feature disentanglement methods from [7] and [8] cannot be extended to cross-domain image classification.

Our new coarse-to-fine domain adaptation method Domain Adaptation via Feature Disentanglement (DAFD) extracts the discriminative features related to classification and eliminates other redundant image features. This reduces the difficulty of feature alignment. The Category-Relevant Feature Selection module CRFS realizes the feature disentanglement in DAFD. With the CRFS, DAFD focuses only on image areas relevant to classification and reduces the attention on category-irrelevant features such as the background. We then introduce the Dynamic Local Maximum Mean Discrepancy module DLMMD for fine-grained alignment. The CRFS guides the DLMMD to focus less on the features irrelevant to classification, thereby improving the domain alignment. Comprehensive experimental results certify the effectiveness of this method for UDA-based cross-domain image classification in multiple domain shift scenarios in comparison to a wide range of the state-of-the-art methods.

Our contribution can be summarized as follows:

- A new cross-domain image classification method called DAFD is proposed. It improves upon the typical discrepancy-based UDA image classification via feature disentanglement. DAFD mitigates the domain shift by using a coarse-to-fine approach and is easy to train.
- We innovatively use the mutual information in our models. Our CRFS distills the category-relevant features, which guides the DLMMD module to focus on discriminative features in the foreground that are most useful for classification while removing background and redundant features.
- Thorough experiments prove the effectiveness of DAFD on several standard UDA image classification datasets. Our method achieves excellent results on these unsupervised image classification tasks.

The remainder of this paper is structured as follows. In Section II, we introduce related works. Our DAFD method is defined in Section III. Section IV presents the experimental results. Finally, our findings and plans for future work are summarized in Section V.

II. Related works

A. Unsupervised Domain Adaptation (UDA)

UDA bridges the domain gap and reduces the domain shift between the source and target domain. UDA methods have achieved excellent results in cross-domain unsupervised image classification [9], [10], image segmentation [11], [12], [13], and object detection [14], [15], [16], [17], [18] by reducing the domain shift at different levels, such as the appearance and feature levels. The research on UDA can be divided into three main lines: discrepancy-based methods, adversarial discriminative models, and self-supervision-based methods. Discrepancy-based methods [19], [20], [21], [22], [23], [24], [25] explicitly measure the discrepancy between two different domains and optimize the network using this discrepancy as a loss. Adversarial discriminative models use an adversarial mechanism to achieve domain confusion [5], [26], [27], [28], [27], [29], [30], [15]. Self-supervision-based methods adopt one or multiple self-supervised tasks to reduce the domain shift [31], [32], [33].

B. UDA for Cross-domain Image Classification

Most of the existing UDA image classification methods are based on convolutional neural networks (CNNs) [34], [35], [36], [37] and transformers [38], [39]. The deep subdomain adaptation network (DSAN) [34] belongs to the discrepancy-based category. DSAN learns to transfer knowledge based on the local maximum mean discrepancy (LMMD) by aligning the subdomain distribution across different domains. DALN [40] learns discriminative and transferable representations while preserving diversity and prediction determinacy. The SCA method [37] considers both the domain and category level with a triplet loss to implement distribution alignment. Zuo *et al.* [41] use the joint distribution of both categories and features to reduce the domain shift. They enlarge the discrepancy among categories by employing a margin-based module to enhance the discrimination of the feature space. Sun *et al.* [42] find that irrelevant features have a negative impact on the knowledge transfer. They align the conditional and marginal probability distributions to transfer knowledge in their ADGFS. Yang *et al.* [38] investigate the transferability of the Vision Transformer (ViT) [43] in UDA image classification. Similarity, in [39], a weight-sharing triple-branch transformer model for source/target feature learning is proposed, which uses self-attention, cross-attention, and feature alignment. The DFA [44] constructs the features of two domains on a common space of Gaussian prior.

C. UDA with Feature Disentanglement

For UDA image classification, a series of feature disentanglement based methods, like [45], [46], [47] use autoencoders to decompose domain-private and domain-shared features. Saito *et al.* [15] reduce the global feature distribution disparity to prevent the network both from focusing on background features and from disregarding foreground features. In [7], a coarse-to-fine approach and an attention-induced feature selection module are proposed to extract the parts relevant to the final classification at a coarse-grained level. More recently, Liu *et al.* [8] create a framework to implement feature disentanglement at local and global levels, improving the feature adaptation ability for UDA-based cross-domain object detection.

We follow this general line of research, but we focus on UDA-based cross-domain image classification using the coarse-to-fine manner with foreground/background feature selection and domain alignment in specific categories.

III. Domain Adaptation via Feature Disentanglement (DAFD)

A. Overview

The purpose of UDA is to transfer the knowledge learned from a labeled source domain to an unlabeled target domain.

We call the source domain Ω_S and target domain Ω_T. The data in source domain be $\Omega_S = (x^s, y^s)$, where $x^s \in X^s$ denotes an image, $y^s \in Y^s$ its category with $Y^s = \{0, 1, 2, \ldots, N\}$ where N is the number of categories. The target domain has the same N categories. We call the data in the target domain $\Omega_T = (x^t, y^t)$ where x^t is an image and y^t is the corresponding label.[1]

We propose the following coarse-to-fine approach for unsupervised domain adaptaion. The structure of our DAFD is shown in Figure 2. The data x^s and x^t are fed into the module during each training iteration. Firstly, the global feature encoder E_g is used to extract the global features. The global features of source and target domain are separately defined as F^s and F^t.

Next, we apply the encoder E_r to obtain the category-relevant features $F^s_{c\_re}$ and $F^t_{c\_re}$. The encoder E_i is used to obtain the category-irrelevant features $F^s_{c\_irre}$ and $F^t_{c\_irre}$.

Then, we use the CRFS module to implement the coarse-grained alignment. In the coarse-grained alignment phase, the CRFS eliminates the features which are not relevant to the image classification (such as the background).

The discriminative features $F^s_{c\_re}$ and $F^t_{c\_re}$ related to classification can still differ between different domains, e.g., due to changes in color or shapes. We apply the DLMMD module to these features to reduce domain shifts at the fine-grained level. Finally, we use a classifier to classify $F^s_{c\_re}$ and $F^t_{c\_re}$. The outputs of the classifier are $\hat{Y}^s$ and $\hat{Y}^t$.

B. Coarse-Grained Alignment: CRFS

The CRFS is designed to pick the features that are most useful for classification (such as the wheels of bikes) and to remove the features that are adverse to the classification (such as the background). Existing methods, such as the UDA-based approach in [31], the adversarial-based DANN [5], and contrast learning [36], mainly focus on aligning all the features of an input image. This alignment does not conform to the properties of image classification tasks. Here, foreground features play a more important role than background features. However, such models likely align features that belong to the background or other features that are useless for classification. Their classifiers are trained with the global features that exhibit noise entanglement with the background and category-irrelevant parts. This makes it difficult to achieve a good classification effect. As remedy, we propose the CRFS module.

We design the category-relevant feature encoder E_r to obtain the category-relevant features $F^s_{c\_re}$ and $F^t_{c\_re}$. The category-irrelevant feature encoder E_i is used to obtain the category-irrelevant features $F^s_{c\_irre}$ and $F^t_{c\_irre}$ to facilitate the feature selection. The two feature encoders are shown in Equations 1 and 2.

$$F^s_{c\_re} = E_r(E(x^s)),\ F^t_{c\_re} = E_r(E(x^t)) \tag{1}$$

$$F^s_{c\_irre} = E_i(E(x^s)),\ F^t_{c\_irre} = E_i(E(x^t)) \tag{2}$$

[1]The labels y^t are not available in an actual application. In our experiments they are known, but *only* to measure the performance. They are not used during training.

We use the two encoders to extract the two kinds of features separately. The mutual information loss $\mathcal{L}_{mi}$ and the image reconstruction loss $\mathcal{L}_{recon}$ are used as the objective function. We aim to minimize this correlation between $F^s_{c\_re}$ and $F^s_{c\_irre}$ as well as $F^t_{c\_re}$ and $F^t_{c\_irre}$. In other words, we seek the minimum of $\mathcal{L}_{mi}$. The definition of mutual information is given in Equation 3, where $H(F^d_{c\_re})$ is the Shannon entropy, $H(F^d_{c\_re}|F^d_{c\_irre})$ is the conditional entropy of $F^d_{c\_re}$ given $F^d_{c\_irre}$, and d represents which domain the data comes from.

$$I(F^d_{c\_re}, F^d_{c\_irre})^d = H(F^d_{c\_re}) - H(F^d_{c\_re}|F^d_{c\_irre}) \tag{3}$$

When d is equal to s and t, the mutual information between category-relevant and category-irrelelant features in the source domain and the target domain is $I(F^s_{c\_re}, F^s_{c\_irre})^s$ and $I(F^t_{c\_re}, F^t_{c\_irre})^t$, respectively. Due to the high dimension of the features, it is difficult to directly calculate the mutual information. So we use MINE [48] to estimate it. Given a distribution $\mathbb{P}$, we denote the empirical distribution associated to n independent identical distributions by $\hat{\mathbb{P}}^{(n)}$. We use M^d for category-relevant feature $F^d_{c\_re}$ and N^d for category-irrelevant feature $F^d_{c\_irre}$.

The optimization method of MINE is defined as Equation 4. $\{T_\theta\}_{\theta\in\Theta}$ is the set of functions parametrized by a neural network.

$$I(M^d; N^d)^d_n = \sup_{\theta\in\Theta} \mathbb{E}_{\mathbb{P}^{(n)}_{M^d N^d}}[T_\theta] - \log\left(\mathbb{E}_{\mathbb{P}^{(n)}_{M^d}\otimes\hat{\mathbb{P}}^{(n)}_{N^d}}\left[e^{T_\theta}\right]\right) \tag{4}$$

We apply the gradient descent approach to maximize Equation 4. The gradient is defined as Equation 5.

$$\hat{G} = \mathbb{E}[\nabla_\theta T_\theta] - \frac{\mathbb{E}[\nabla_\theta T_\theta e^{T_\theta}]}{\mathbb{E}[e^{T_\theta}]} \tag{5}$$

Algorithm 1 MINE

1: Initialize the network parameters θ;
2: **repeat**
3: Draw b minibatch samples from the joint distribution: $(m^{(1)}, n^{(1)}), \ldots, (m^{(b)}, n^{(b)}) \sim \mathbb{P}_{M^d N^d}$;
4: Draw b samples from the marginal distribution N^d: $\bar{n}^{(1)}, \ldots, \bar{n}^{(b)} \sim \mathbb{P}^d_N$
5: Evaluate the lower-bound: $V(\theta) \leftarrow \frac{1}{b}\sum_{i=1}^{b} T_\theta(m^{(i)}, n^{(i)}) - \log(\frac{1}{b}\sum_{i=1}^{b} e^{T_\theta(m^{(i)}, \bar{n}^{(i)})})$
6: Evaluate bias-corrected gradients (e.g., moving average): $\hat{G}(\theta) \leftarrow \widetilde{\nabla}_\theta \mathcal{V}(\theta)$
7: Update the statistic network parameters: $\theta \leftarrow \theta + \hat{G}(\theta)$
8: **until** convergence

We execute MINE (Algorithm 1) once per iteration at training time to obtain a mutual information estimator. The mutual information loss is defined as Equation 6.

$$\mathcal{L}^d_{mi}(M^d; N^d)_n = \mathbb{E}_{\mathbb{P}^{(n)}_{M^d N^d}}[T_\theta] - \log\left(\mathbb{E}_{\mathbb{P}^{(n)}_{M^d}\otimes\hat{\mathbb{P}}^{(n)}_{N^d}}\left[e^{T_\theta}\right]\right) \tag{6}$$

After training the mutual information estimator, we can use it to calculate the mutual information between F_{c_re} and

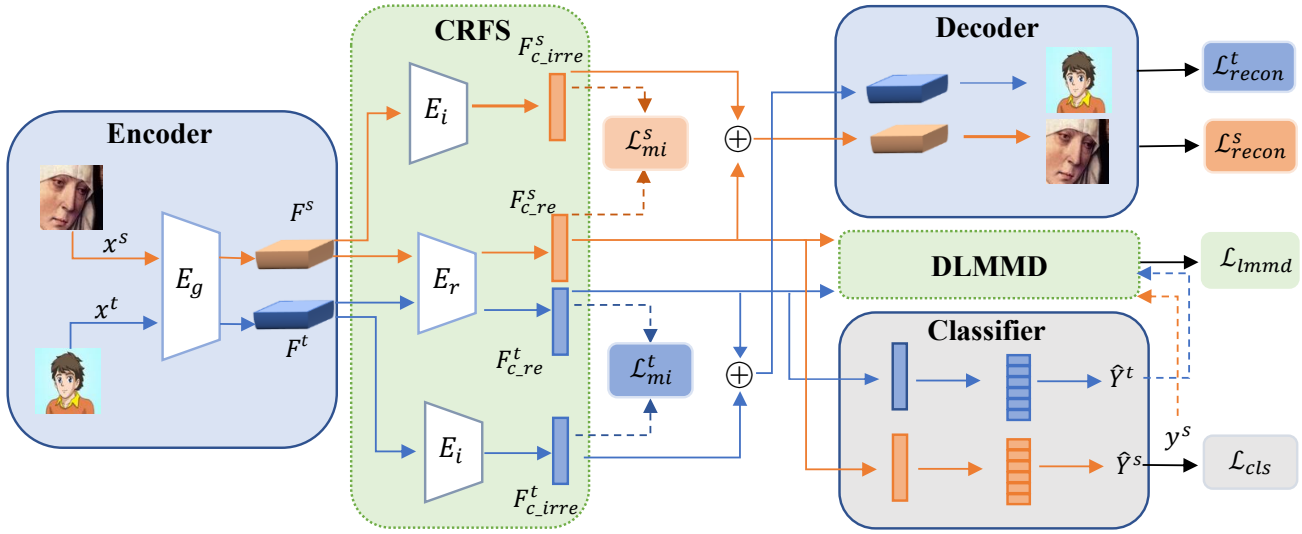

Fig. 2. The architecture of our DAFD method. x^s and x^t represent the source and target images, respectively. DAFD consists of two modules: the category-relevant feature selection module and the dynamic local maximum mean discrepancy module. We reduce the domain shifts in a coarse-to-fine schedule by combing the CRFS and the DLMMD. We feed the source and target image into the encoder E_g to get global features. Then, these global features are fed into the CRFS module to get the discriminative features $F^s_{c\_re}$ and $F^t_{c\_re}$ for classification and the category-irrelevant features $F^s_{c\_irre}$ and $F^t_{c\_irre}$. Finally, the DLMMD module is used to reduce the discrepancy between the different domains for these discriminative features at category level. The outputs of the classifier are $\hat{Y}^s$ and $\hat{Y}^t$.

F_{c_irre} as a loss function. However, the network may aim to minimize the mutual information by generating a meaningless, maybe random, vector F_{c_irre}, rather than features extracted from images. Then, the model cannot achieve the purpose of feature disentanglement. Therefore, we use the reconstruction loss $\mathcal{L}_{recon}$ to constrain F_{c_irre}. $\mathcal{L}_{recon}$ is defined in Equations 7 and 8, where x^{s_recon} and x^{t_recon} are the output of decoder. N_s and N_t represent the number of samples from the source and target domain, respectively. μ is the number of pixels of the input and output images and $\|\cdot\|_2^2$ is the squared L_2-norm.

$$\mathcal{L}^s_{recon}(x^s, x^{s\_recon}) = \frac{1}{N_s}\sum_{i=1}^{N_s}\frac{1}{\mu}\|(x_i^s - x_i^{s\_recon})\|_2^2 \quad (7)$$

$$\mathcal{L}^t_{recon}(x^t, x^{t\_recon}) = \frac{1}{N_t}\sum_{i=1}^{N_t}\frac{1}{\mu}\|(x_i^t - x_i^{t\_recon})\|_2^2 \quad (8)$$

C. Fine-Grained Alignment: DLMMD

It is not enough to simply use our CRFS module for coarse-grained domain alignment. After we distill the discriminative features F_{c_re} related to classification, there are still differences (such as color and shape) between these features on different domains. We now reduce the domain shift between these features. Following [34], we propose the DLMMD as a fine-grained alignment method in our model.

1) Subdomain alignment: The most direct method for this purpose is to minimize the discrepancy of different domains. However, this incorrectly brings different categories of images closer to each other in feature space, which affects the alignment. As shown in Figure 3, images of the same category act as subdomains. The DLMMD achieves category-level feature alignment by aligning different subdomains separately from the fine-grained level. By minimizing the discrepancy of different subdomains, we can achieve category-level alignment. The corresponding loss function is defined as Equation 9, where w_i^{sc} and w_j^{tc} denote the weight of x_i^s and x_j^t belonging to class c. We compute w_c^i for the sample x_i as Equation 10, where y_{ic} is the c-th entry of vectory y_i and y_i is a one-hot vector. The source domain data is with real labels. The target domain is with the probability distribution predicted by the network.

2) Pseudo labels of target images: Subdomain alignment requires obtaining labels for the target domain. To address this problem, we use the category distribution of the data output by the classifier in the network to generate the labels for the target domain. We use the category with the highest prediction probability as a pseudo-label for the data. However, we now face a new problem: Images with low predicted score could have the opposite effect because the network misaligns the different categories. We therefore adopt a strategy to improve the accuracy of the pseudo-labels. We only select data whose probability value exceeds a threshold K to generate pseudo-labels. With each iteration, we dynamically select the new data to generate pseudo-labels. Compared with DSAN [34], this can improve the stability of the network training early on. It reduces the interference of low-confidence images at the early stage of training.

$$\mathcal{L}_{lmmd} = \frac{1}{C}\sum_{c=1}^{C}\Big\| \sum_{x_i^s \in X^s} \omega_i^{sc} E_r(E(x_i^s)) - \sum_{x_j^t \in X^t} \omega_j^{tc} E_r(E(x_j^t)) \Big\|_{\mathcal{H}}^2 \quad (9)$$

$$w_i^c = \frac{y_{ic}}{\sum_{(x_j, y_j)\in X} y_{jc}} \quad (10)$$

D. Network Optimization

Our DAFD contains three modules in the training stage: the classifier, the CRFS, and the DLMMD. The classifier is

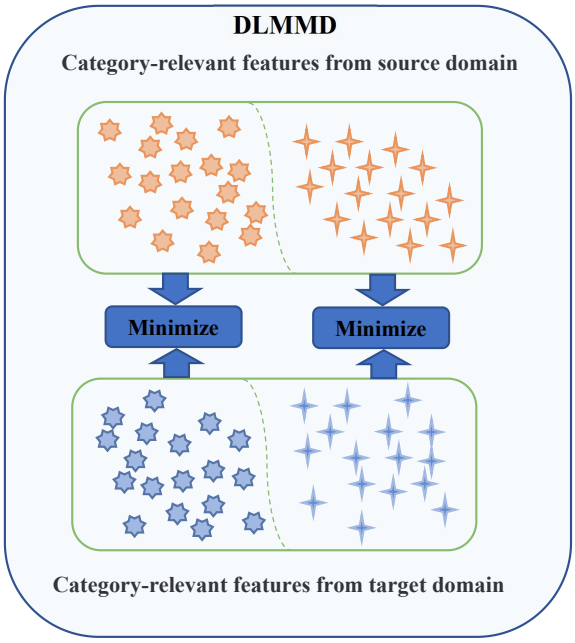

Fig. 3. The structure of DLMMD. Category-relevant features are obtained by Equation 1. Graphics of the same shape and different colors represent features of the same category in different domains. Features of the same category in all domains form a subdomain. Since the labels of the target domain cannot be used at training time, we use the output of the classification layer to create pseudo-labels for the images of the target domain. We minimize Equation 9 between source and target features with same category.

for final image classification and the *cross-entropy* loss $\mathcal{L}_{cls}$ is used as the classification loss.

$$\mathcal{L}_{cls} = \mathbb{E}_{(x_i^s, y_i^s)} \mathcal{L}_{CE}(C(E_r(x_i^s)), y_i^s) \tag{11}$$

The overall loss of the DAFD is:

$$\mathcal{L}_{DAFD} = \mathcal{L}_{cls} + \lambda_1 \mathcal{L}_{lmmd} + \lambda_2(\mathcal{L}_{recon}^s + \mathcal{L}_{recon}^t) + \lambda_3(\mathcal{L}_{mi}^s + \mathcal{L}_{mi}^t) \tag{12}$$

where λ_1, λ_2, and λ_3 are hyperparameters. During network optimization, the mutual information estimator MINE is trained alternatingly with the entire network.

IV. Experiment

A. Experimental Setup

A good domain adaptation method should be robust and work well for different applications. We therefore investigate two very different use cases: cross-domain image classification and digit recognition.

The datasets Office-31 [49] and Office-Home [3] are used for image classification. MNIST [50] and USPS [51] are used for digit recognition.

Office-31 is a benchmark dataset for UDA image classification with 4110 images of 31 categories and the three domains Webcam (W), DSLR (D), and Amazon (A). We test all of the six possible transfer tasks W→A, A→D, W→D, D→W, D→A and A→W.

Office-Home is another benchmark dataset for UDA image classification. It has 15,500 images, 65 categories, and the four domains Clip Art (Cl), Artistic (Ar), Real-World (Rw), and Product (Pr). We investigate all of the twelve possible transfer tasks.

MNIST and USPS: We utilize two digit datasets, USPS and MNIST, to investigate the knowledge transfer for digit recognition. There are 70,000 pictures of size 28*28 in the MNIST dataset. The USPS dataset has 20,000 pictures and an image size of 16*16. Both datasets have ten categories. We test both transfer tasks, USPS→MNIST and MNIST→USPS.

For cross-domain image classification, all images all resized to 224*224 pixels and we employ ResNet50 [52] as backbone. For digit recognition, we use LeNet [53] as backbone. SGD is used as the optimizer for the model parameters. Its momentum and weight decay are set to 0.9 and 0.005, respectively. We set the probability threshold K for the pseudo-labels to 0.8. Random image flipping and cropping are adopted. We implement DAFD in PyTorch. In the inference process, the DLMMD module is not used.

In order to prevent noise from interfering with the network during the early stages of training, λ_1 gradually increases from 0 to 1. In order to stabilize the mutual information estimator during the early stage of the training, we gradually change λ_3 from 0 to 1 as well. Otherwise, F_{c_re} and F_{c_irre} would update too quickly too early for the estimator training to converge. We fix λ_2 at 1.

B. Comparison With Existing Methods

First, we compare our method with the baseline, i.e., the network that we modify (ResNet50 [52] or LeNet [53]) without any domain adaptation technique. Our approach is an improvement and innovation based on DSAN [34], so it is necessary to compare with it as well. As representatives for adversarial-based UDA methods, DANN [5], CDAN [26], CDAN+E [26], and ADDA [10] were chosen. SCA [37] is included because it also uses a discrepancy-based approach to achieve domain alignment. Although ADGFS [42] uses a completely different technology from us, the ideas are somewhat similar, so we also compare with it. DALN [40] is very recent and it has excellent performance. Finally, DFA [44] is another recent method.

The experimental results are shown in Tables I, II, and III. We marked the highest accuracy with bold face and underlined the second highest accuracy in each task.

Firstly we find that our DAFD outperforms DSAN on Office-31, Office-Home, MNIST→USPS, and USPS→MNIST. The corresponding improvements of the average accuracy are 1.4%, 1.9%, 0.8%, and 0.5%. The reason is that DSAN aligns not only discriminative features related to classification, but also background features or redundant features on the foreground. This can have a negative impact on domain alignment. The CRFS module that we propose solves this problem. Our model has improved accuracy relative to DSAN, which proves that our method is effective.

Secondly, our DAFD outperforms most of the existing methods on most tasks. The average accuracy of DAFD on Office-31, Office-Home, MNIST→USPS, and USPS→MNIST are 89.8%, 69.5%, 97.7%, and 95.8%. Although the mean

TABLE I
ACCURACY (%) ON OFFICE-31 FOR UNSUPERVISED DOMAIN ADAPTATION (USING RESNET-50 AS THE BACKBONE/BASELINE).

Method	A→W	D→W	W→D	A→D	D→A	W→A	Avg
Baseline [52]	68.4	96.7	99.3	68.9	62.5	60.7	76.1
DANN [5]	82.0	96.9	99.1	79.7	68.2	67.4	82.2
ADGFS [42]	85.9	98.1	99.8	88.4	70.6	74.8	86.3
CDAN [26]	93.1	98.2	**100.0**	89.8	70.1	68.0	86.6
CDAN+E [26]	94.1	98.6	**100.0**	92.9	71.0	69.3	87.7
SCA [37]	93.6	98.0	**100.0**	89.5	72.6	72.4	87.7
DSAN [34]	93.6	98.3	**100.0**	90.2	73.5	74.8	88.4
DFA [44]	93.5	**99.4**	**100.0**	94.8	73.8	71.0	88.8
DALN [40]	**95.2**	99.1	**100.0**	**95.4**	**76.4**	**76.5**	**90.4**
Basel.+CRFS	84.2	97.6	**100.0**	85.5	68.6	65.9	83.6
Basel.+CRFS+DLMMD	94.1	98.1	**100.0**	93.9	**76.4**	**76.5**	89.8

TABLE II
ACCURACY (%) ON OFFICE-HOME FOR UNSUPERVISED DOMAIN ADAPTATION (USING RESNET-50 AS THE BACKBONE/BASELINE).

Method	Ar→Cl	Ar→Pr	Ar→Rw	Cl→Ar	Cl→Pr	Cl→Rw	Pr→Ar	Pr→Cl	Pr→Rw	Rw→Ar	Rw→Cl	Rw→Pr	Avg
Baseline [52]	34.9	50.0	58.0	37.4	41.9	46.2	38.5	31.2	60.4	53.9	41.2	59.9	46.1
DANN [5]	45.6	59.3	70.1	47.0	58.5	60.9	46.1	43.7	68.5	63.2	51.8	76.8	57.6
SCA [37]	46.7	64.6	71.3	53.1	65.3	65.2	54.6	47.2	72.7	68.2	56.0	80.2	62.1
CDAN [26]	49.0	69.3	74.5	54.4	66.0	68.4	55.6	48.3	75.9	68.4	55.4	80.5	63.8
CDAN+E [26]	50.7	70.6	76.0	57.6	70.0	70.0	57.4	50.9	77.3	70.9	56.7	81.6	65.8
DSAN [34]	54.4	70.8	75.4	60.4	67.8	68.0	62.6	55.9	78.5	73.8	60.6	83.1	67.6
DFA [44]	52.8	73.9	77.4	**66.5**	72.9	73.6	64.9	53.1	78.7	**74.5**	58.1	82.4	69.1
DALN [40]	**57.8**	**79.9**	**82.0**	66.3	**76.2**	**77.2**	**66.7**	55.5	**81.3**	73.5	60.4	**85.3**	**71.8**
Basel.+CRFS	51.4	68.9	74.8	56.0	65.8	67.1	55.7	46.4	76.3	66.2	53.6	79.5	63.5
Basel.+CRFS+DLMMD	56.6	74.1	77.6	63.2	71.4	70.3	64.8	**56.6**	80.1	74.2	**61.4**	83.9	69.5

TABLE III
ACCURACY (%) ON DIGIT RECOGNITION TASKS FOR UNSUPERVISED DOMAIN ADAPTATION (USING LENET AS THE BACKBONE/BASELINE). "-" MEANS THAT THE EXPERIMENTAL RESULTS OF THE METHOD ON THIS DATASET WERE NOT AVAILABLE.

Method	MNIST→USPS	USPS→MNIST
Baseline [53]	75.2	57.1
DANN [5]	77.1	73.0
ADDA [10]	89.4	90.1
DSAN [34]	96.9	95.3
SCA [37]	96.1	95.5
DALN [40]	-	-
DFA [44]	**98.6**	**96.6**
Basel.+CRFS	82.2	70.6
Basel.+CRFS+DLMMD	97.7	95.8

accuracy of our method is slightly lower than that of the best method (DALN) on the Office-31 and Office-Home datasets, DALN is an adversarial learning network, while we do not use the adversarial paradigm in our method. Therefore, our network is easier to train.

On the digit recognition tasks, DFA [44] performs slightly better that our approach, but by no more than 1% in average accuracy. However, the relationship between the feature induced from the classifier and the latent feature is ignored in DFA, which could limit transferability of this model. From the experimental results on much more complicated datasets, i.e., Office-31 and Office-Home, we find that our method is actually better.

Thirdly, our method performs better on datasets with large size images (Office-31 and Office-Home), i.e., there is more improvement over DSAN and there is less improvement in small-sized datasets (MNIST and USPS). On one hand, the domain gap between MNIST and USPS may be smaller. On the other hand, in MNIST and USPS, the foreground part tends to occupy a larger part of the entire image, that is, there are fewer redundant features. Conversely, on datasets containing large-sized images, the background differs more significantly between the different domains, and the foreground contains more redundant features.

To make this comparison fair, we only apply the loss from Equation 9 to the last layer of E_r, which is the same as in DSAN. Since these data are obtained from multiple datasets, this certifies the validity and robustness of our model.

(a) Original (b) Baseline (c) Baseline + CRFS

Fig. 4. Visualization of model attention using the CAM technique in the training. Given an input image (a), the attention variance caused by the CRFS is illustrated in (c). We observe that Basel. + CRFS could strengthen the learning of discriminative features while reducing background noise. Basel. + CRFS focuses more on the wheels of the bike and ignores the biker's legs and other background features. This helps to reduce the difficulty of feature alignment in the DLMMD module to improve the effect of domain alignment.

C. Ablation Study

We empirically verify the effectiveness of each module in DAFD via both visualization and statistics. Firstly, we set the regularization parameters to zero by removing the DLMMD module in DAFD. We find that the accuracy on all three datasets is improved compared to not using the CRFS. The underlying principle of our CRFS is illustrated in Figure 4. We visualize the attention of the model using the Class Activation Mapping (CAM) technique [54]. Originally, the model activates the wheels of the bike, human legs, and some background for recognition (Figure 4(b)). The activation map yielded by the ResNet50 with CRFS shown in Figure 4(c) focuses on the wheels (more representative for the bike) and the activation from the background and the human legs is reduced. These removed features tend to vary greatly from domain to domain. The background and the human legs are redundant. If the network focuses on these features, the effectiveness of domain alignment is reduced. Conversely, if the network focuses on features that are more critical to classification, and those features are similar across domains (for example, the wheels of a bicycle), the knowledge transfer is improved.

We now demonstrate our conclusions based on the training loss. Figure 5(a) shows that when training the ResNet50 model, the classification loss gradually decreases and converges, but there is almost no change in $\mathcal{L}_{LMMD}$. This indicates that the discrepancy between the source and the target domain does not decrease with training. In Figure 5(b), we only use the CRFS module for domain alignment, under which the LMMD loss is not involved in optimization. As the training progresses, the LMMD loss gradually decreases and eventually converges. This shows that the process of feature selection will also reduce the discrepancy between the two domains.

Secondly, when the CRFS and DLMMD modules are combined, a higher classification accuracy can be achieved compared to DSAN. The reason is that the fine-grained alignment module DLMMD only needs to focus on the discriminative features relevant to classification. This reduces the effect of category-irrelevant features on the knowledge transfer. Figure 6(a) shows the loss in the training of our DAFD network.

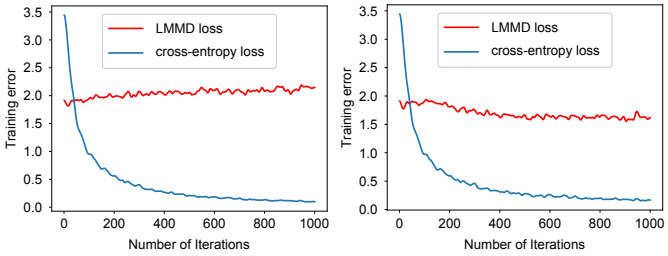

(a) ResNet50 (b) ResNet50 with CRFS

Fig. 5. Results on A→D on Office-31 using ResNet50 and ResNet50 with CRFS. In (a) and (b), the red lines represent the LMMD loss $\mathcal{L}_{LMMD}$ and the blue lines represent the classification loss $\mathcal{L}_{CLS}$. Even though $\mathcal{L}_{LMMD}$ does not participate in training, it is still gradually decreasing and converges in (b), which indicates that the DRFS module can reduce the gap between different domains. In contrast, the LMMD loss does not change significantly in (a).

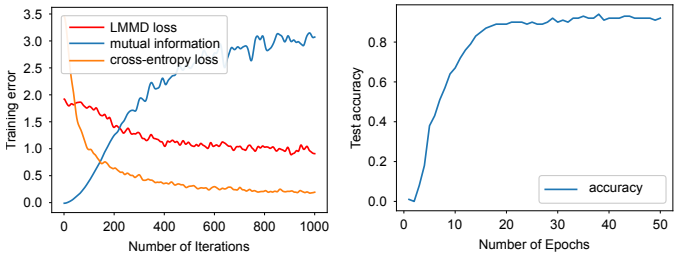

(a) A→D training loss on Office-31 (b) classification accuracy of DAFD

Fig. 6. Results on A→D of Office-31 using the DAFD on $A \rightarrow D$ of Office-31: Since the mutual information estimator and CRFS module are trained alternatingly, the mutual information loss will gradually increase and eventually converge. From (b), we find that the test accuracy gradually increases, which shows that our model is stable.

Figure 6(b) shows the accuracy of the classifier. As can be seen, our network is easy to train. The accuracy and loss converge quickly, and the training process is stable, which proves the stability of our network training.

At last, the above conclusions can also be confirmed by t-SNE [55] visualization in Figure 7. These plots visualize high-dimensional data by giving each data point a location in a two dimensional map. The CRFS and DLMMD modules proposed by us is designed for domain alignment of coarse-

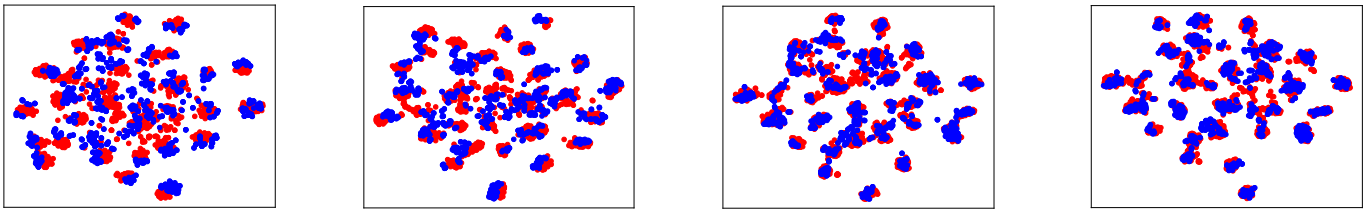

(a) Basel. (b) Basel. + CRFS (c) Basel.+ DLMMD (d) Basel. + CRFS + DLMMD

Fig. 7. t-SNE [55] visualization for task **A**→**D** on Office-31 dataset. Red and blue points indicate the source and the target domain, respectively. From left to right: (a) baseline (source images only), (b) coarse-grained alignment with CRFS, (c) fine-grained alignment with DLMMD, and (d) the full system (DAFD).

grained and fine-grained features, respectively. It can be seen from the Figures 7(b) and 7(c) that both modules can achieve domain alignment respectively. When we combine the CRFS and the DLMMD module, the two domains are aligned better: the data points from source and target domain are very close to each other. This demonstrates the effectiveness of our method.

V. Conclusion

In this paper, we propose Domain Adaptation via Feature Disentanglement (DAFD) as a new model for unsupervised domain adaptation. We use a Category-relevant Feature Selection (CRFS) module to distill the discriminative features for classification and then we use a Dynamic Local Maximum Mean Discrepancy (DLMMD) module to reduce the discrepancy between different domains. Comprehensive experiments on four benchmark datasets demonstrate the effectiveness of the proposed model. It can significantly increase the performance of the networks into which it is integrated. This allows it to outperform the majority of the state-of-the-art on the field.

In our future work, we will explore other, better ways of feature disentanglement to obtain better results. We will also apply our methods to other scenarios, such as object detection. Finally, we will also seek to combine our method with the related work DALN.

Acknowledgments

We acknowledge support from the Key Research Plan of Anhui 2022k07020011 and 202104d07020006, the open fund of Information Materials and Intelligent Sensing Laboratory of Anhui Province IMIS202205, the University Natural Sciences Research Project of Anhui Province KJ2020A0661, the National Natural Science Foundation of China under grant 61673359, the Key Common Technology and Major Scientific Achievement Engineering Project of Hefei 2021GJ030, as well as the Hefei Specially Recruited Foreign Expert program.

References

[1] A. Torralba and A. A. Efros, "Unbiased look at dataset bias," in *Proceedings of the 24th IEEE Conference on Computer Vision and Pattern Recognition (CVPR'11), Jun. 20-25, 2011, Colorado Springs, CO, USA*. Los Alamitos, CA, USA: IEEE Computer Society, 2011, pp. 1521–1528. [Online]. Available: https://doi.org/10.1109/CVPR.2011.5995347

[2] M. Wang and W. Deng, "Deep visual domain adaptation: A survey," *Neurocomputing*, vol. 312, pp. 135–153, 2018. [Online]. Available: https://doi.org/10.1016/j.neucom.2018.05.083

[3] H. Venkateswara, J. Eusebio, S. Chakraborty, and S. Panchanathan, "Deep hashing network for unsupervised domain adaptation," in *Proceedings of the 2017 IEEE Conference on Computer Vision and Pattern Recognition (CVPR'17), Jul. 21-26, 2017, Honolulu, HI, USA*. Los Alamitos, CA, USA: IEEE Computer Society, 2017, pp. 5385–5394. [Online]. Available: https://doi.org/10.1109/CVPR.2017.572

[4] M. Long, Y. Cao, J. Wang, and M. I. Jordan, "Learning transferable features with deep adaptation networks," in *Proceedings of the 32nd International Conference on Machine Learning (ICML'15), Jul. 6-11, 2015 Lille, France*, ser. JMLR Workshop and Conference Proceedings, F. R. Bach and D. M. Blei, Eds., vol. 37. NE, USA: JMLR.org, 2015, pp. 97–105. [Online]. Available: http://proceedings.mlr.press/v37/long15.html

[5] Y. Ganin, E. Ustinova, H. Ajakan, P. Germain, H. Larochelle, F. Laviolette, M. Marchand, and V. S. Lempitsky, "Domain-adversarial training of neural networks," in *Domain Adaptation in Computer Vision Applications*, ser. Advances in Computer Vision and Pattern Recognition, G. Csurka, Ed. Berlin/Heidelberg, Germany: Springer, 2017, pp. 189–209. [Online]. Available: https://doi.org/10.1007/978-3-319-58347-1_10

[6] M. Arjovsky, S. Chintala, and L. Bottou, "Wasserstein generative adversarial networks," in *Proceedings of the 34th International Conference on Machine Learning (ICML'17), Aug. 6-11, 2017 Sydney, NSW, Australia*, ser. Proceedings of Machine Learning Research, D. Precup and Y. W. Teh, Eds., vol. 70. NE, USA: PMLR, 2017, pp. 214–223. [Online]. Available: http://proceedings.mlr.press/v70/arjovsky17a.html

[7] H. Zhang, G. Luo, J. Li, and F.-Y. Wang, "C2FDA: Coarse-to-fine domain adaptation for traffic object detection," *IEEE Transactions on Intelligent Transportation Systems*, vol. 23, no. 8, pp. 12 633–12 647, 2022. [Online]. Available: https://doi.org/10.1109/TITS.2021.3115823

[8] D. Liu, C. Zhang, Y. Song, H. Huang, C. Wang, M. Barnett, and W. Cai, "Decompose to adapt: Cross-domain object detection via feature disentanglement," *CoRR*, vol. abs/2201.01929, 2022. [Online]. Available: https://arxiv.org/abs/2201.01929

[9] Y. Ganin and V. S. Lempitsky, "Unsupervised domain adaptation by backpropagation," in *Proceedings of the 32nd International Conference on Machine Learning (ICML'15), Jul. 6-11, 2015 Lille, France*, ser. JMLR Workshop and Conference Proceedings, F. R. Bach and D. M. Blei, Eds., vol. 37. NE, USA: JMLR.org, 2015, pp. 1180–1189. [Online]. Available: http://proceedings.mlr.press/v37/ganin15.html

[10] E. Tzeng, J. Hoffman, K. Saenko, and T. Darrell, "Adversarial discriminative domain adaptation," in *Proceedings of the 2017 IEEE Conference on Computer Vision and Pattern Recognition (CVPR'17), Jul. 21-26, 2017, Honolulu, HI, USA*. Los Alamitos, CA, USA: IEEE Computer Society, 2017, pp. 2962–2971. [Online]. Available: https://doi.org/10.1109/CVPR.2017.316

[11] Y. Li, L. Yuan, and N. Vasconcelos, "Bidirectional learning for domain adaptation of semantic segmentation," in *Proceedings of the IEEE Conference on Computer Vision and Pattern Recognition (CVPR'19), Jun. 16-20, 2019, Long Beach, CA, USA*. Piscataway, NJ, USA: Computer Vision Foundation / IEEE, 2019, pp. 6936–6945. [Online]. Available: https://doi.org/10.1109/CVPR.2019.00710

[12] T. Vu, H. Jain, M. Bucher, M. Cord, and P. Pérez, "ADVENT: adversarial entropy minimization for domain adaptation in semantic segmentation," in *Proceedings of the IEEE Conference on Computer Vision and Pattern Recognition (CVPR'19), Jun. 16-20, 2019, Long Beach, CA, USA*. Piscataway, NJ, USA: Computer Vision Foundation / IEEE, 2019, pp. 2517–2526. [Online]. Available: https://doi.org/10.1109/CVPR.2019.00262

[13] D. Liu, D. Zhang, Y. Song, F. Zhang, L. O'Donnell, H. Huang, M. Chen, and W. Cai, "Unsupervised instance segmentation in microscopy images via panoptic domain adaptation and task re-weighting," in *Proceedings of the 2020 IEEE/CVF Conference on Computer Vision and Pattern Recognition (CVPR'20), Jun. 13-19, 2020, Seattle, WA, USA*. Piscataway, NJ, USA: Computer Vision Foundation / IEEE, 2020, pp. 4242–4251. [Online]. Available: https://doi.org/10.1109/CVPR42600.2020.00430

[14] Y. Chen, W. Li, C. Sakaridis, D. Dai, and L. V. Gool, "Domain adaptive faster R-CNN for object detection in the wild," in *Proceedings of the 2018 IEEE Conference on Computer Vision and Pattern Recognition (CVPR'18), Jun. 18-22, 2018, Salt Lake City, UT, USA*. Los Alamitos, CA, USA: Computer Vision Foundation / IEEE Computer Society, 2018, pp. 3339–3348. [Online]. Available: https://doi.org/10.1109/CVPR.2018.00352

[15] K. Saito, Y. Ushiku, T. Harada, and K. Saenko, "Strong-weak distribution alignment for adaptive object detection," in *Proceedings of the IEEE Conference on Computer Vision and Pattern Recognition (CVPR'19), Jun. 16-20, 2019, Long Beach, CA, USA*. Piscataway, NJ, USA: Computer Vision Foundation / IEEE, 2019, pp. 6956–6965. [Online]. Available: https://doi.org/10.1109/CVPR.2019.00712

[16] Z. He and L. Zhang, "Domain adaptive object detection via asymmetric tri-way Faster-RCNN," in *Proceedings of the 16th European Conference on Computer Vision (ECCV'20), Aug. 23-28, 2020, Glasgow, UK, Part XXIV*, ser. LNCS, A. Vedaldi, H. Bischof, T. Brox, and J. Frahm, Eds., vol. 12369. Berlin/Heidelberg, Germany: Springer, 2020, pp. 309–324. [Online]. Available: https://doi.org/10.1007/978-3-030-58586-0_19

[17] X. Zhu, J. Pang, C. Yang, J. Shi, and D. Lin, "Adapting object detectors via selective cross-domain alignment," in *Proceedings of the IEEE Conference on Computer Vision and Pattern Recognition (CVPR'19), Jun. 16-20, 2019, Long Beach, CA, USA*. Piscataway, NJ, USA: Computer Vision Foundation / IEEE, 2019, pp. 687–696. [Online]. Available: https://doi.org/10.1109/CVPR.2019.00078

[18] C. Chen, Z. Zheng, X. Ding, Y. Huang, and Q. Dou, "Harmonizing transferability and discriminability for adapting object detectors," in *Proceedings of the 2020 IEEE/CVF Conference on Computer Vision and Pattern Recognition (CVPR'20), Jun. 13-19, 2020, Seattle, WA, USA*. Piscataway, NJ, USA: Computer Vision Foundation / IEEE, 2020, pp. 8866–8875. [Online]. Available: https://doi.org/10.1109/CVPR42600.2020.00889

[19] J. Zhuo, S. Wang, W. Zhang, and Q. Huang, "Deep unsupervised convolutional domain adaptation," in *Proceedings of the 2017 ACM on Multimedia Conference (MM'17), Oct. 23-27, 2017 Mountain View, CA, USA*, Q. Liu, R. Lienhart, H. Wang, S. K. Chen, S. Boll, Y. P. Chen, G. Friedland, J. Li, and S. Yan, Eds. New York, NY, USA: ACM, 2017, pp. 261–269. [Online]. Available: https://doi.org/10.1145/3123266.3123292

[20] B. Wu, X. Zhou, S. Zhao, X. Yue, and K. Keutzer, "SqueezeSegV2: Improved model structure and unsupervised domain adaptation for road-object segmentation from a LiDAR point cloud," in *Proceedings of the International Conference on Robotics and Automation (ICRA'19), May 20-24, 2019, Montreal, QC, Canada*. Piscataway, NJ, USA: IEEE, 2019, pp. 4376–4382. [Online]. Available: https://doi.org/10.1109/ICRA.2019.8793495

[21] W. Zellinger, T. Grubinger, E. Lughofer, T. Natschläger, and S. Saminger-Platz, "Central moment discrepancy (CMD) for domain-invariant representation learning," in *Proceedings of the 5th International Conference on Learning Representations (ICLR'17), Apr. 24-26, 2017, Toulon, France*. Toronto, ON, Canada: OpenReview.net, 2017, also: arXiv CoRR abs/1702.08811. [Online]. Available: http://arxiv.org/abs/1702.08811

[22] Y. Li, N. Wang, J. Shi, X. Hou, and J. Liu, "Adaptive batch normalization for practical domain adaptation," *Pattern Recognition*, vol. 80, pp. 109–117, 2018. [Online]. Available: https://doi.org/10.1016/j.patcog.2018.03.005

[23] F. M. Carlucci, L. Porzi, B. Caputo, E. Ricci, and S. R. Bulò, "AutoDIAL: Automatic domain alignment layers," in *Proceedings of the IEEE International Conference on Computer Vision (ICCV'17), Oct. 22-29, 2017, Venice, Italy*. Los Alamitos, CA, USA: IEEE Computer Society, 2017, pp. 5077–5085. [Online]. Available: https://doi.org/10.1109/ICCV.2017.542

[24] A. Rozantsev, M. Salzmann, and P. Fua, "Beyond sharing weights for deep domain adaptation," *IEEE Transactions on Pattern Analysis and Machine Intelligence*, vol. 41, no. 4, pp. 801–814, 2019. [Online]. Available: https://doi.org/10.1109/TPAMI.2018.2814042

[25] G. Kang, L. Jiang, Y. Yang, and A. G. Hauptmann, "Contrastive adaptation network for unsupervised domain adaptation," in *Proceedings of the IEEE Conference on Computer Vision and Pattern Recognition (CVPR'19), Jun. 16-20, 2019, Long Beach, CA, USA*. Piscataway, NJ, USA: Computer Vision Foundation / IEEE, 2019, pp. 4893–4902. [Online]. Available: https://doi.org/10.1109/CVPR.2019.00503

[26] M. Long, Z. Cao, J. Wang, and M. I. Jordan, "Conditional adversarial domain adaptation," in *Advances in Neural Information Processing Systems 31: Proceedings of the Annual Conference on Neural Information Processing Systems 2018 (NeurIPS'18), Dec. 3-8, 2018, Montréal, Canada*, S. Bengio, H. M. Wallach, H. Larochelle, K. Grauman, N. Cesa-Bianchi, and R. Garnett, Eds. New Orleans, LA, USA: Neural Information Processing Systems Foundation, Inc., 2018, pp. 1647–1657.

[27] Y. Du, Z. Tan, Q. Chen, X. Zhang, Y. Yao, and C. Wang, "Dual adversarial domain adaptation," *CoRR*, vol. abs/2001.00153, 2020. [Online]. Available: http://arxiv.org/abs/2001.00153

[28] S. Cicek and S. Soatto, "Unsupervised domain adaptation via regularized conditional alignment," in *Proceedings of the 2019 IEEE/CVF International Conference on Computer Vision (ICCV'2019), Oct. 27-Nov. 2, 2019, Seoul, Korea (South)*. Piscataway, NJ, USA: IEEE, 2019, pp. 1416–1425. [Online]. Available: https://doi.org/10.1109/ICCV.2019.00150

[29] M. Xu, J. Zhang, B. Ni, T. Li, C. Wang, Q. Tian, and W. Zhang, "Adversarial domain adaptation with domain mixup," in *Proceedings of the 34th AAAI Conference on Artificial Intelligence (AAAI'20), The 32nd Innovative Applications of Artificial Intelligence Conference (IAAI'20), The 10th AAAI Symposium on Educational Advances in Artificial Intelligence (EAAI'20), Feb. 7-12, 2020, New York, NY, USA*. AAAI Press, 2020, pp. 6502–6509. [Online]. Available: https://doi.org/10.1609/aaai.v34i04.6123

[30] Z. He and L. Zhang, "Multi-adversarial Faster-RCNN for unrestricted object detection," in *Proceedings of the 2019 IEEE/CVF International Conference on Computer Vision (ICCV'2019), Oct. 27-Nov. 2, 2019, Seoul, Korea (South)*. Piscataway, NJ, USA: IEEE, 2019, pp. 6667–6676. [Online]. Available: https://doi.org/10.1109/ICCV.2019.00677

[31] F. M. Carlucci, A. D'Innocente, S. Bucci, B. Caputo, and T. Tommasi, "Domain generalization by solving jigsaw puzzles," in *Proceedings of the IEEE Conference on Computer Vision and Pattern Recognition (CVPR'19), Jun. 16-20, 2019, Long Beach, CA, USA*. Piscataway, NJ, USA: Computer Vision Foundation / IEEE, 2019, pp. 2229–2238.

[32] J. Xu, L. Xiao, and A. M. López, "Self-supervised domain adaptation for computer vision tasks," *IEEE Access*, vol. 7, pp. 156 694–156 706, 2019. [Online]. Available: https://doi.org/10.1109/ACCESS.2019.2949697

[33] Z. Feng, C. Xu, and D. Tao, "Self-supervised representation learning from multi-domain data," in *Proceedings of the 2019 IEEE/CVF International Conference on Computer Vision (ICCV'2019), Oct. 27-Nov. 2, 2019, Seoul, Korea (South)*. Piscataway, NJ, USA: IEEE, 2019, pp. 3244–3254. [Online]. Available: https://doi.org/10.1109/ICCV.2019.00334

[34] Y. Zhu, F. Zhuang, J. Wang, G. Ke, J. Chen, J. Bian, H. Xiong, and Q. He, "Deep subdomain adaptation network for image classification," *IEEE Transactions on Neural Networks and Learning Systems*, vol. 32, no. 4, pp. 1713–1722, 2021. [Online]. Available: https://doi.org/10.1109/TNNLS.2020.2988928

[35] Y. Ganin, E. Ustinova, H. Ajakan, P. Germain, H. Larochelle, F. Laviolette, M. Marchand, and V. S. Lempitsky, "Domain-adversarial training of neural networks," *Journal of Machine Learning Research*, vol. 17, pp. 59:1–59:35, 2016. [Online]. Available: http://jmlr.org/papers/v17/15-239.html

[36] J. Huang, D. Guan, A. Xiao, S. Lu, and L. Shao, "Category contrast for unsupervised domain adaptation in visual tasks," in *Proceedings of the IEEE/CVF Conference on Computer Vision and Pattern Recognition (CVPR'22), Jun. 18-24, 2022, New Orleans, LA, USA*. Piscataway, NJ, USA: IEEE, 2022, pp. 1193–1204. [Online]. Available: https://doi.org/10.1109/CVPR52688.2022.00127

[37] W. Deng, L. Zheng, Y. Sun, and J. Jiao, "Rethinking triplet loss for domain adaptation," *IEEE Transactions on Circuits and Systems for Video Technology*, vol. 31, no. 1, pp. 29–37, 2021. [Online]. Available: https://doi.org/10.1109/TCSVT.2020.2968484

[38] J. Yang, J. Liu, N. Xu, and J. Huang, "TVT: transferable vision transformer for unsupervised domain adaptation," *CoRR*, vol. abs/2108.05988, 2021. [Online]. Available: https://arxiv.org/abs/2108.05988

[39] T. Xu, W. Chen, P. Wang, F. Wang, H. Li, and R. Jin, "CDTrans: Cross-domain transformer for unsupervised domain adaptation," in *Proceedings of the 10th International Conference on Learning Representations (ICLR'22), Apr. 25-29, 2022, Virtual Event*. Toronto, ON, Canada: OpenReview.net, 2022, also: arXiv CoRR abs/2109.06165. [Online]. Available: https://arxiv.org/abs/2109.06165

[40] L. Chen, H. Chen, Z. Wei, X. Jin, X. Tan, Y. Jin, and E. Chen, "Reusing the task-specific classifier as a discriminator: Discriminator-free adversarial domain adaptation," in *Proceedings of the IEEE/CVF Conference on Computer Vision and Pattern Recognition (CVPR'22), Jun. 18-24, 2022, New Orleans, LA, USA*. Piscataway, NJ, USA: IEEE, 2022, pp. 7171–7180. [Online]. Available: https://doi.org/10.1109/CVPR52688.2022.00704

[41] Y. Zuo, H. Yao, L. Zhuang, and C. Xu, "Margin-based adversarial joint alignment domain adaptation," *IEEE Transactions on Circuits and Systems for Video Technology*, vol. 32, no. 4, pp. 2057–2067, 2022. [Online]. Available: https://doi.org/10.1109/TCSVT.2021.3081729

[42] J. Sun, Z. Wang, W. Wang, H. Li, F. Sun, and Z. Ding, "Joint adaptive dual graph and feature selection for domain adaptation," *IEEE Transactions on Circuits and Systems for Video Technology*, vol. 32, no. 3, pp. 1453–1466, 2022. [Online]. Available: https://doi.org/10.1109/TCSVT.2021.3073937

[43] A. Dosovitskiy, L. Beyer, A. Kolesnikov, D. Weissenborn, X. Zhai, T. Unterthiner, M. Dehghani, M. Minderer, G. Heigold, S. Gelly, J. Uszkoreit, and N. Houlsby, "An image is worth 16x16 words: Transformers for image recognition at scale," in *Proceedings of the 9th International Conference on Learning Representations (ICLR'21), May 3-7, 2021, Virtual Event, Austria*. Toronto, ON, Canada: OpenReview.net, 2021, also: arXiv CoRR abs/2010.11929. [Online]. Available: https://arxiv.org/abs/2010.11929

[44] J. Wang, J. Chen, J. Lin, L. Sigal, and C. W. de Silva, "Discriminative feature alignment: Improving transferability of unsupervised domain adaptation by gaussian-guided latent alignment," *Pattern Recognition*, vol. 116, p. 107943, 2021. [Online]. Available: https://doi.org/10.1016/j.patcog.2021.107943

[45] K. Bousmalis, G. Trigeorgis, N. Silberman, D. Krishnan, and D. Erhan, "Domain separation networks," in *Advances in Neural Information Processing Systems 29: Proceedings of the Annual Conference on Neural Information Processing Systems 2016, (NeurIPS'16), Dec. 5-10, 2016, Barcelona, Spain*, D. D. Lee, M. Sugiyama, U. von Luxburg, I. Guyon, and R. Garnett, Eds. New Orleans, LA, USA: Neural Information Processing Systems Foundation, Inc., 2016, pp. 343–351.

[46] R. Cai, Z. Li, P. Wei, J. Qiao, K. Zhang, and Z. Hao, "Learning disentangled semantic representation for domain adaptation," in *Proceedings of the 28th International Joint Conference on Artificial Intelligence (IJCAI'19), Aug. 10-16, 2019, Macao, China*, S. Kraus, Ed. ijcai.org, 2019, pp. 2060–2066. [Online]. Available: https://doi.org/10.24963/ijcai.2019/285

[47] X. Peng, Z. Huang, X. Sun, and K. Saenko, "Domain agnostic learning with disentangled representations," in *Proceedings of the 36th International Conference on Machine Learning (ICML'19), Jun. 9-15, 2019, Long Beach, California, USA*, ser. Proceedings of Machine Learning Research, K. Chaudhuri and R. Salakhutdinov, Eds., vol. 97. NE, USA: PMLR, 2019, pp. 5102–5112. [Online]. Available: http://proceedings.mlr.press/v97/peng19b.html

[48] M. I. Belghazi, A. Baratin, S. Rajeswar, S. Ozair, Y. Bengio, R. D. Hjelm, and A. C. Courville, "Mutual information neural estimation," in *Proceedings of the 35th International Conference on Machine Learning (ICML'18), Jul. 10-15, 2018, Stockholmsmässan, Stockholm, Sweden*, ser. Proceedings of Machine Learning Research, J. G. Dy and A. Krause, Eds., vol. 80. NE, USA: PMLR, 2018, pp. 530–539. [Online]. Available: http://proceedings.mlr.press/v80/belghazi18a.html

[49] K. Saenko, B. Kulis, M. Fritz, and T. Darrell, "Adapting visual category models to new domains," in *Proceedings of the 11th European Conference on Computer Vision (ECCV'10), Sep. 5-11, 2010, Heraklion, Crete, Greece, Part IV*, ser. LNCS, K. Daniilidis, P. Maragos, and N. Paragios, Eds., vol. 6314. Berlin/Heidelberg, Germany: Springer, 2010, pp. 213–226. [Online]. Available: https://doi.org/10.1007/978-3-642-15561-1_16

[50] Y. LeCun, L. Bottou, Y. Bengio, and P. Haffner, "Gradient-based learning applied to document recognition," *Proceedings of the IEEE*, vol. 86, no. 11, pp. 2278–2324, 1998. [Online]. Available: https://doi.org/10.1109/5.726791

[51] Y. Netzer, T. Wang, A. Coates, A. Bissacco, B. Wu, and A. Y. Ng, "Reading digits in natural images with unsupervised feature learning," 2011. [Online]. Available: https://ai.stanford.edu/~twangcat/papers/nips2011_housenumbers.pdf

[52] K. He, X. Zhang, S. Ren, and J. Sun, "Deep residual learning for image recognition," in *Proceedings of the 2016 IEEE Conference on Computer Vision and Pattern Recognition (CVPR'16), Jun. 27-30, 2016, Las Vegas, NV, USA*. Los Alamitos, CA, USA: IEEE Computer Society, 2016, pp. 770–778. [Online]. Available: https://doi.org/10.1109/CVPR.2016.90

[53] Y. LeCun, B. E. Boser, J. S. Denker, D. Henderson, R. E. Howard, W. E. Hubbard, and L. D. Jackel, "Handwritten digit recognition with a back-propagation network," in *Advances in Neural Information Processing Systems 2, Proceedings of the NIPS Conference, Nov. 27-30, 1989, Denver, CO, USA*, D. S. Touretzky, Ed. Morgan Kaufmann, 1989, pp. 396–404.

[54] B. Zhou, A. Khosla, À. Lapedriza, A. Oliva, and A. Torralba, "Learning deep features for discriminative localization," in *Proceedings of the 2016 IEEE Conference on Computer Vision and Pattern Recognition (CVPR'16), Jun. 27-30, 2016, Las Vegas, NV, USA*. Los Alamitos, CA, USA: IEEE Computer Society, 2016, pp. 2921–2929. [Online]. Available: https://doi.org/10.1109/CVPR.2016.319

[55] L. van der Maaten and G. E. Hinton, "Visualizing data using t-SNE," *Journal of Machine Learning Research*, vol. 9, no. 86, pp. 2579–2605, 2008. [Online]. Available: http://jmlr.org/papers/v9/vandermaaten08a.html